J Appl Physiol 130: 298–307, 2021.
First published December 10, 2020; doi:10.1152/japplphysiol.00232.2020

american physiological society

JOURNAL OF APPLIED PHYSIOLOGY

RESEARCH ARTICLE

Breath-hold task induces temporal heterogeneity in electroencephalographic regional field power in healthy subjects

Maria Sole Morelli,[1,2] Nicola Vanello,[3] Alejandro Luis Callara,[4] Valentina Hartwig,[5] Michelangelo Maestri,[6] Enrica Bonanni,[6] Michele Emdin,[1,2] Claudio Passino,[1,2] and Alberto Giannoni[1,2]

[1]*Scuola Superiore Sant'Anna, Pisa, Italy;* [2]*Fondazione Toscana Gabriele Monasterio, Pisa, Italy;* [3]*Department of Information Engineering, University of Pisa, Pisa, Italy;* [4]*University of Pisa School of Engineering, Centro di Ricerca "E. Piaggio", Pisa, Italy;* [5]*Institute of Clinical Physiology, National Council of Research, Pisa, Italy; and* [6]*Departement of Neuroscience, University of Pisa, Pisa, Italy*

Abstract

We demonstrated that changes in CO_2 values cause oscillations in the cortical activity in δ-and α-bands. The analysis of the regional field power (RFP) showed evidence that different cortical areas respond with different time delays to CO_2 challenges. An opposite behavior was found for the end-tidal O_2. We suppose that the different cortical time delays likely expresse specific ascending pathways to the cortex, generated by chemoreceptor nuclei in the brain stem. Although the brain stem is in charge of the automatic control of ventilation, the cortex is involved in the voluntary control of breathing but also receives inputs from the brain stem, which influences the perception of breathing, the arousal state and sleep architecture in conditions of hypoxia/hypercapnia. We evaluated in 11 healthy subjects the effects of breath hold (BH; 30 s of apneas and 30 s of normal breathing) and BH-related CO_2/O_2 changes on electroencephalogram (EEG) global field power (GFP) and RFP in nine different areas (3 rostrocaudal sections: anterior, central, and posterior; and 3 sagittal sections: left, middle, and right) in the δ- and α-bands by cross correlation analysis. No significant differences were observed in GFP or RFP when comparing free breathing (FB) with the BH task. Within the BH task, the shift from apnea to normal ventilation was accompanied by an increase in the δ-power and a decrease in the α-power. The end-tidal pressure of CO_2 ($P_{ET}CO_2$) was positively correlated with the δ-band and negatively with the α- band with a positive time shift, whereas an opposite behavior was found for the end-tidal pressure of O_2 ($P_{ET}O_2$). Notably, the time shift between $P_{ET}CO_2$ / $P_{ET}O_2$ signals and cortical activity at RFP was heterogenous and seemed to follow a hierarchical activation, with the δ-band responding earlier than the α-band. Overall, these findings suggest that the effect of BH on the cortex may follow specific ascending pathways from the brain stem and be related to chemoreflex stimulation.

NEW & NOTEWORTHY We demonstrated that the end tidal CO_2 oscillation causes oscillations of delta and alpha bands. The analysis of the regional field power showed that different cortical areas respond with different time delays to CO_2 challenges. An opposite behavior was found for the end-tidal O_2. We can suppose that the different cortical time delay response likely expresses specific ascending pathways to the cortex generated by chemoreceptor nuclei in the brainstem.

chemoreflex; EEG; hypercapnia; hypoxia; neural pathways; respiration

INTRODUCTION

Spontaneous breathing in mammals is a complex function under automatic control of the brain stem neural network (1). This network originates in the medulla, receives inputs both from the periphery and the cortex, and is responsible for the background respiratory rhythm and the coupling of oxygen (O_2) consumption and carbon dioxide (CO_2) production to metabolic needs, a function known as chemosensitivity (2).

CO_2 is the primary chemical stimulus for alveolar ventilation and is mainly sensed by the central chemoreceptors (70–80% of CO_2 response in condition of normoxia). These receptors are mainly located in the medulla and respond to pH and CO_2 variations so that in the condition of hypercapnia they cause an increase in ventilation resetting CO_2 and pH to steady-state levels. On the other hand, peripheral chemoreceptors, located in the carotid bodies in humans, are mainly responsible for O_2 levels and the sensing of hypoxia but also respond to CO_2 (20–30% of CO_2 response in the condition of normoxia) and pH variations (3, 4).

Beyond their effects on ventilation and the autonomic outflow, the chemoreflex is known to have influences also on the cortex through specific ascending pathways (5, 6). Tracking this pathway is not only physiologically but also clinically relevant, since it is involved in the perception of breathing (i.e., dyspnea), and alertness during wakefulness

Correspondence: M. S. Morelli (e-mail: msmorelli@monasterio.it).
Submitted 30 March 2020 / Revised 5 November 2020 / Accepted 4 December 2020

or arousability during sleep, and it is implicated in conditions associated with oscillatory ventilation such as obstructive sleep apnea (OSA) and central apneas (CA). Moreover, the possibility to pharmacologically or surgically modulate the chemoreflex has recently emerged in sleep disorder breathing, hypertension, and heart failure (7–12), and thus there might be the need to explore the effects of these novel interventions on cortical activity.

In this respect, the effects of CO_2/O_2 variations on brain activity have been explored mainly by using electroencephalography (EEG) (13–19). In humans, hypercapnia is known to cause an increase in the EEG global field power (GFP) in the δ-band (1–4 Hz) as well as a reduction in the α-band (8–13 Hz) (14, 15, 18, 19). This suggests that, during hypercapnia, brain activity resembles a low-arousal state (18, 19). Similar results were observed in conditions of asphyxia, such as those induced by chocking, in which hypercapnia is accompanied by a various degree of hypoxia (20).

Variations in CO_2 and O_2 arterial levels may be experimentally induced either by administering different gas mixtures or by voluntary breath hold (BH). Despite also having some effects on cortical motor/sensory activity, BH has the advantage to be easy to perform, without requiring a specific device with respect to gas administration (21). BH initially requires conscious inhibition by the cortex of the brain stem network but then allows a progressive increase in CO_2 and decrease in O_2, mimicking the respiratory dynamics of OSA and CA (22). In those conditions, a sinusoidal increase in CO_2 and decrease in O_2 is usually observed differently from the square wave increase to nonphysiological O_2/CO_2 values generally obtained by gas administration. However, to stress the chemoreflex system in the right range of perturbation, the respiratory cycle time is fundamental, since the average apnea length of OSA/CA is ~30 s (23–25). Previous studies have used longer (80–225 s) or shorter (10 s) voluntary BH intervals (26, 27). The cross-correlation between EEG GFP in δ-band and end-tidal CO_2 ($P_{ET}CO_2$) during 30 s of BH has been recently explored by our group, with the finding that the variation of $P_{ET}CO_2$ usually precedes the variations observed in the GFP (14). However, by looking at GFP, it is not possible to comprehend whether different cortical areas respond to gas challenges in a different fashion.

This is of physiological interest, since if the cortex is responding to stimulation of the different group of chemoreceptors during gas challenges, some heterogeneous temporo-spatial distribution of neural response is likely to occur. Indeed, different chemoreceptors usually operate around different response thresholds and with different time delays and have specific neuroanatomic connections with the cortex (28–31). On the other hand, CO_2/O_2 changes may cause effects on cortical activity by either vasodilation or direct neural activation independently from chemoreflex recruitment. If this alternative hypothesis is correct, a rather uniform and homogeneous variation in cortical activity is to be expected. While it is impossible to unravel this question by looking at EEG GFP, the use of regional field power (RFP) analysis may instead shed light on this topic.

Therefore, in the current study, we aimed at studying by cross-correlation analysis the cortical regional variations of EEG RFP in the δ- and α-bands related to hypercapnia and hypoxia induced by voluntary BH in healthy subjects.

MATERIALS AND METHODS

Eleven healthy subjects (all males, age 30 ± 6 yr) were recruited for the study. Six subjects were derived from a previous study by our group in which only EEG GFP changes in the δ-band induced by BH were investigated and related to $P_{ET}CO_2$ (14), and thus this study is partly a reanalysis of previous data. However, a larger population was enrolled in the current study, focusing this time on the effects of BH on EEG RFP. Furthermore, the effects of $P_{ET}O_2$ and the changes observed in the α-band were incorporated in the analysis differently from our previous work.

A 64-electrode EEG device was used (Compumedics Neuroscan, SynAmps RT) to record brain signals. Simultaneously with EEG acquisition, exhaled CO_2, O_2, and blood oxygen saturation (Sp_{O_2}) were recorded with a gas analyzer (Cosmoplus; Novametrics) and a pulse oximeter (Pulsox-7; Minolta), respectively.

Two different tasks were performed. In the free-breathing (FB) task, subjects had to breathe normally for 6 min while lying down with their eyes closed. In the BH task, the subjects had to breathe normally for 1 min and then alternate 30 s of BH performed after normal inspiration to 30 s of normal breathing for five cycles for a total of 6 min of acquisition, still with their eyes closed. Subjects were advised to start or stop the BH by touching their left leg. The same touching procedure was used during the FB task to control for somatosensory potential confounders due to the instructions given to the subject.

The experimental protocol was approved by the Institutional Ethics Committee (Comitato Etico Area Vasta Nord-Ovest, Pisa, Italy). The recordings were carried out in agreement with the Declaration of Helsinki. Written, informed consent was obtained from all subjects.

EEG Analysis

EEG signal analysis was already described (14). Briefly, all channels were re-referenced to average signals, and channels with low signal-to-noise ratio were excluded from the analysis. The impedance of all electrodes was checked and kept below 30 kΩ during all recordings to ensure a good signal quality. EEG signals underwent baseline correction, Hann pass band filter (1–30 Hz), blink and cardiac artefacts detection, and removal using a principal component analysis (PCA) method (32). The global measure of EEG power was expressed as GFP and the regional distribution of the EEG power in different brain areas was obtained as RFP for the δ (1–3 Hz)- and α (8–13 Hz)-bands. Specifically, for RFP, nine areas were extracted, dividing the scalp into three different sections [left (L), middle (M), and right (R)] and further dividing into three rostrocaudal sections [anterior (A), central (C), and posterior (P)] (15).

Physiological Signal Processing

The physiological signals were processed as described (14). Briefly, Sp_{O_2} was used to detect possible effects induced by the tasks on oxygen levels. The normal range of Sp_{O_2} was considered to lie between 95% and 100%. The exhaled CO_2 and O_2 waveforms were used to estimate the $P_{ET}CO_2$ and $P_{ET}O_2$ time series, respectively, as an estimate of arterial CO_2 and O_2 (33). Because no exhalation of CO_2/O_2 occurs during the voluntary

apnea phase, the $P_{ET_{CO_2}}$ and $P_{ET_{O_2}}$ signals were estimated by using a cubic spline model interpolating $P_{ET_{CO_2}}$ and $P_{ET_{O_2}}$ found before and after the cessation of breathing.

Cross-Correlation Analysis

The cross-correlation function (CCF) was used to evaluate the similarity between $P_{ET_{CO_2}}$ / $P_{ET_{O_2}}$ and EEG power (both GFP and RFP) as a function of different time lags. The CCFs were estimated using a previously described method (34). Briefly, the peak of CCF and the corresponding time lag were evaluated. In our analysis, if the maximum correlation occurred for negative time shift, the EEG power signal was considered to lead the $P_{ET_{CO_2}}$ / $P_{ET_{O_2}}$ signal. On the other hand, if the maximum correlation occurred for positive time shift, the $P_{ET_{CO_2}}$ / $P_{ET_{O_2}}$ signal was considered to lead to the EEG signal. The CCF was estimated for time lags between −30 s and 30 s as proposed (35). Furthermore, the weighted average CCFs were also estimated in the group of subjects under study.

Statistical Analysis

Variations in $P_{ET_{CO_2}}$ / $P_{ET_{O_2}}$ and RFP between the two tasks (FB and BH) were estimated by comparing their medians with a nonparametric Wilcoxon signed-rank test (36), with the null hypothesis (H0) being that the differences between FB and BH tasks came from a distribution with zero median. A comparison between the phase of voluntary apnea and that of normal breathing within the BH task was also performed with a nonparametric Wilcoxon signed-rank test (36). In order to assess at the group level how cross-correlation between $P_{ET_{CO_2}}$ / $P_{ET_{O_2}}$ and GFP or RFP varied between the two tasks (i.e., FB and BH), we compared their weighted average cross-correlation values with a nonparametric Wilcoxon signed-rank test under the null hypothesis (H0) of no differences between the tasks. We controlled false discovery rate through the Benjamini-Yekuteli correction for multiple testing under dependency (37, 38). We assessed the statistical significance of cross-correlation analysis by means of a phase randomization approach (39). Specifically, for each subject, we generated n = 1,000 surrogates of $P_{ET_{CO_2}}$ / $P_{ET_{O_2}}$ and EEG δ-power and α-power (both global and regional) under the null hypothesis of no correlation between the time series. Specifically, such surrogates preserved original time series magnitude, but with a randomly distributed phase in range (0,2π). Then, we evaluated the cross-correlation between surrogate time series. Accordingly, at regional analysis, we obtained for each scalp region (s), for each frequency (f), and for each time lag (t) a surrogate distribution of cross-correlation under the null hypothesis of absence of correlation. Then, we associated with each observed cross-correlation (s, f, and t) a P value based on its position in the surrogate distribution. The same procedure was repeated for GFP analysis for each frequency and for each time lag. Finally, we controlled multiple testing (α = 0.05) with the false discovery rate procedure described (37, 38). Accordingly, we obtained the critical P value at which tests were considered significant.

RESULTS

An oscillatory behavior with larger variations in both $P_{ET_{CO_2}}$ and $P_{ET_{O_2}}$ was documented during BH as compared with FB [coefficient of variation (CV) for $P_{ET_{CO_2}}$: BH 7.1% vs. FB 2.2%, P = 0.001; CV for $P_{ET_{O_2}}$: BH 8.8% vs. FB 2.6%, P = 0.008]. No significant changes were observed in the Sp_{O_2} signal between the two tasks (CV for Sp_{O_2}: FB 1.1% vs. CV BH; 0.7%, P = 0.11), and thus $P_{ET_{O_2}}$ rather than Sp_{O_2} was used for subsequent analyses.

The signal behavior during FB and BH tasks in a sample subject for GFP in δ and α bands, $P_{ET_{CO_2}}$ and $P_{ET_{O_2}}$ is provided in Supplemental Fig. S1 (all Supplemental Material for this article can be found online at https://doi.org/10.6084/m9.figshare.12040578.v3), whereas the GFP average values in the whole group of subjects between FB and BH and, within the BH task, between the phases of apnea and normal breathing are provided in Supplemental Table S1. The time courses of the CCFs estimated at group level for GFP during the FB and BH tasks for $P_{ET_{CO_2}}$ and $P_{ET_{O_2}}$ are provided in Supplemental Fig. S2 and Supplemental Table S2 as well as Supplemental Fig. S3 and Supplemental Table S3, respectively. As for $P_{ET_{CO_2}}$, a positive correlation with the δ-band and a negative correlation with the α-band were observed for a positive time shift, whereas the opposite behavior was instead observed for $P_{ET_{O_2}}$.

Spectral Maps and Regional Field Power Analysis

When comparing FB with the BH task considered as a whole, no significant differences were observed in the EEG spectral maps (Table 1 and Fig. 1). Conversely, within the BH task, an increase in the δ-power and a decrease in the α-power were observed after the apnea phase (Table 1 and Fig. 1). More precisely, at the spectral maps, the same behavior was observed in all regions but RA and RC in the δ-band and LA, RA, RC, and RP in the in the α-band (Table 1 and Fig. 1). Each one of the nine regions included in the EEG analysis had at least two channels, since the average number of electrodes removed from the analysis was 3 ± SD, and the spatial distribution of excluded electrodes was sparse.

The CCFs for the nine cortical areas during FB and BH tasks for both the δ- and α-bands are shown in Fig. 2 for $P_{ET_{CO_2}}$ and in Fig. 3 for $P_{ET_{O_2}}$. During FB, the CCFs between $P_{ET_{CO_2}}$ and RFP and $P_{ET_{O_2}}$ and RFP were not significant. On the contrary, within the BH task, the CCF between $P_{ET_{CO_2}}$ and RFP was found to be positive in the δ-band and negative in the α-band for positive time shifts in all regions but RP for the δ-band (not significant) and RA, RC, and RP for the α-band (positive correlations) (Table 2 and Fig. 2*B*). The CCF between $P_{ET_{O_2}}$ and RFP was found instead to be negative in the δ-band and positive in the α-band for positive time shifts in all cases but RA and RP for the δ-band (positive correlations) (Table 3 and Fig. 3*B*).

Notably, a different phase shift in the $P_{ET_{CO_2}}$ concentration waveform and the EEG power waveform was observed in the different cortical regions [see Supplemental Video S1]. In particular, in the δ-band an earlier activation in the MA and MC (2 s of delay) was observed, with the LA, LC, MP showing the highest EEG delay (ranging from 7 to 9 s). In the α-band, an even more heterogeneous behavior of cortical time responses to $P_{ET_{CO_2}}$ variations among different regions was observed, with the right regions (RA, RC, and RP) usually showing negative time delays and positive correlations differently from the medial and left regions, showing

Table 1. *EEG power spectra in δ- and α-bands in 9 different regions*

	δ-Band					α-Band				
	FB	BH	*P* value	Apnea in BH	Respiration in BH	*P* value	FB	BH	*P* value	Apnea in BH	Respiration in BH	*P* value
Left anterior	1.02 ± 0.15	0.98 ± 0.04	0.76	0.99 ± 0.05*	1.10 ± 0.10*	0.001*	0.96 ± 0.08	0.96 ± 0.08	0.92	0.99 ± 0.10	0.95 ± 0.10	0.06
Middle anterior	1.05 ± 0.18	1.01 ± 0.05	0.76	1.02 ± 0.05*	1.09 ± 0.09*	0.06*	0.99 ± 0.13	0.96 ± 0.08	0.32	0.98 ± 0.10*	0.93 ± 0.09*	0.02*
Right anterior	0.09 ± 0.08	0.09 ± 0.04	1.00	1.00 ± 0.06	1.09 ± 0.10	0.10	0.97 ± 0.07	0.98 ± 0.08	1.00	1.02 ± 0.12	0.96 ± 0.09	0.08
Left central	1.01 ± 0.09	1.01 ± 0.05	0.32	1.02 ± 0.06*	1.14 ± 0.18*	0.006*	0.95 ± 0.07	0.97 ± 0.08	0.77	1.01 ± 0.11*	0.95 ± 0.10*	0.04*
Middle central	0.98 ± 0.05	0.99 ± 0.08	0.62	1.01 ± 0.08	1.06 ± 0.10	0.06	0.96 ± 0.09	0.96 ± 0.04	1.00	0.98 ± 0.05*	0.92 ± 0.05*	0.04*
Right central	0.97 ± 0.07	0.98 ± 0.07	0.69	0.99 ± 0.08*	1.09 ± 0.09*	0.002*	0.98 ± 0.10	0.95 ± 0.08	0.62	0.98 ± 0.13	0.92 ± 0.07	0.06
Left posterior	0.98 ± 0.09	1.00 ± 0.09	0.37	1.01 ± 0.11*	1.19 ± 0.29*	0.002*	0.95 ± 0.13	0.96 ± 0.07	0.92	0.98 ± 0.09*	0.93 ± 0.10*	0.04*
Middle posterior	1.00 ± 0.08	0.96 ± 0.11	0.43	0.96 ± 0.11*	1.09 ± 0.09*	0.002*	0.92 ± 0.09	0.93 ± 0.06	0.92	0.96 ± 0.08*	0.89 ± 0.09*	0.05*
Right posterior	0.99 ± 0.14	0.98 ± 0.08	0.56	0.98 ± 0.10*	1.09 ± 0.11*	0.009*	0.89 ± 0.12	0.93 ± 0.09	0.55	0.96 ± 0.11	0.90 ± 0.09	0.08

Values are means ± SD. BH, breath hold; FB, free breathing. Comparisons between the FB and BH task were considered. Furthermore, in the BH task, a comparison between respiratory phases and apnea phases was performed. *Significant difference ($P < 0.05$).

instead positive time delays and negative correlations. In the latter regions, a longer time shift and a lower time dispersion were documented in the α-band as compared with the δ-band (range: 14–16 s vs. 2–9 s) (Fig. 2*B* and Table 2). A similar trend with an opposite sign was observed for CCFs between $P_{ET_{O_2}}$ and RFP (Fig. 3*B* and Table 3 as well as Supplemental Video S2).

DISCUSSION

In this study, the cortical responses to BH were evaluated in healthy subjects, both globally (average across all electrodes) and, for the first time, in nine different regions (3 rostrocaudal sections: anterior, central, and posterior; and 3 sagittal sections: left, middle, and right) for two frequency bands of interest (i.e., δ- and α-bands). No significant changes were observed in the cortical activity by comparing FB with BH, but within the BH maneuver a significant variation was observed by comparing the apnea phase with the normal ventilation phase. Notably, $P_{ET_{CO_2}}$ was positively correlated with the δ-band and negatively with the α-band (apart from the right regions) for positive time shifts, whereas $P_{ET_{O_2}}$ was negatively correlated with the δ-band and positively correlated with the α-band. This is logical considering the counterphase oscillation of $P_{ET_{CO_2}}$ and $P_{ET_{O_2}}$ during the two phases of BH. Most importantly, a different time shift between $P_{ET_{CO_2}}$ and $P_{ET_{O_2}}$ envelopes and the EEG RFP signal in the nine cortical regions was observed, suggesting that the effect of BH on the cortex may follow the specific ascending pathway from the brain stem due to chemoreflex stimulation.

Although coherent and significant trends were observed across all subjects, we reported only the results of the analysis at group level, which are more consistent, considering the simulated test results (14) and the observed percentage of missing data segments in each subject. Our findings are in line with previous studies, in which an increase in the δ-band and a reduction in the α-band was found throughout the whole brain in the hypercapnic condition (18, 19). Similar findings were also observed in patients with spontaneous apneas, such as patients with OSA and CA (40, 41) Interestingly, in the study by Wang et al. (18), three different conditions were compared: *1*) hyperoxic/hypercapnia, *2*) hypoxic-hypercapnia, and *3*) normocapnic/hypoxia. Both hyperoxic/hypercapnia and hypoxic/hypercapnia led to an increase in the δ-band power and to a decrease in the α-band, without any significant difference between the two trials. Most notably, hypoxic/normocapnia had no effect on the two bands. These findings suggest that CO_2, rather than O_2, seems the main driver of EEG changes also during BH.

Considering that BH is a complex task, which also involves, beyond task-related oscillations in the respiratory gases, a change in the motor and sensory cortical activity, we cannot exclude that the observed changes may be due to the task commitment rather than the observed gas variations. However, considering that similar results were obtained by gas administration (18, 19) and observed in spontaneous apneas (40, 41), this potential interpretation seems less likely, although it cannot be completely excluded, especially when RFP analysis is taken into consideration.

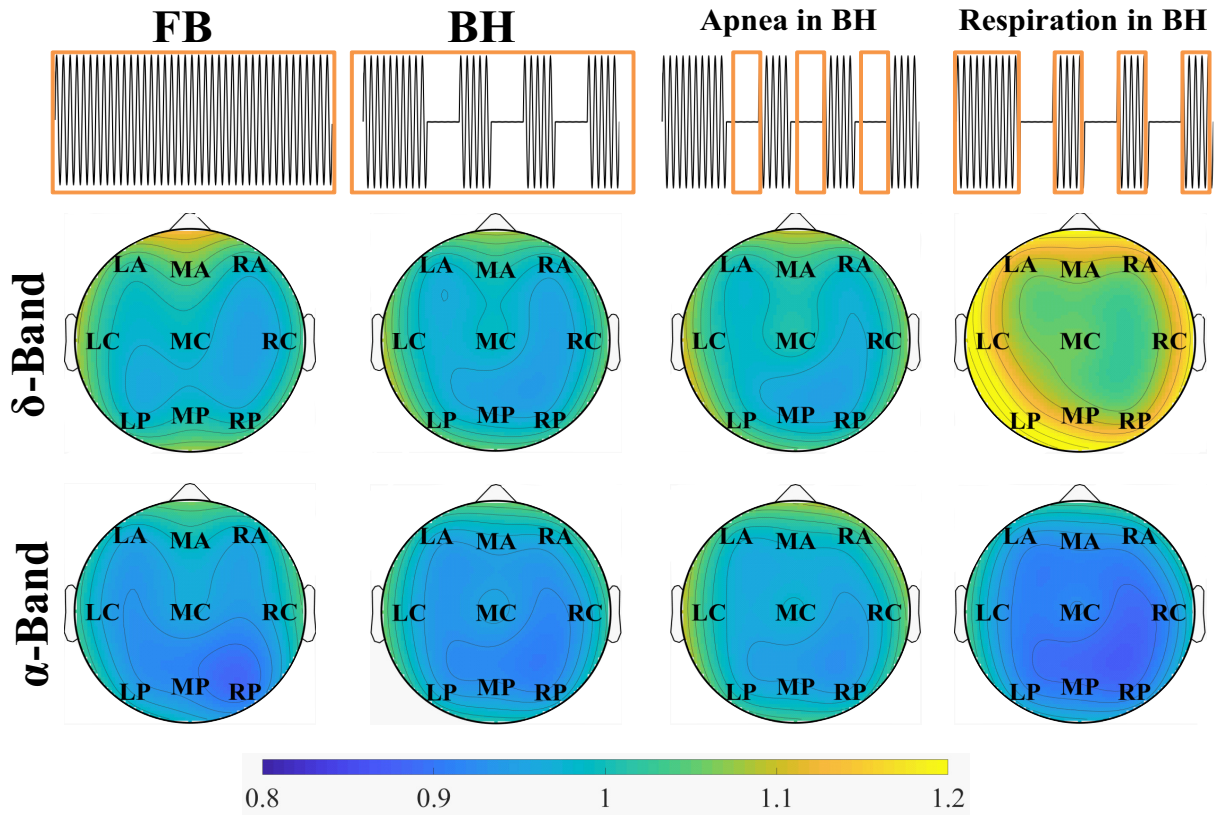

Figure 1. Electroencephalography (EEG) spectral maps in δ- and α-bands. Four different conditions are shown: *1*) free-breathing (FB) task, *2*) breath-hold (BH) task; *3*) apnea phase within BH task, and *4*) respiratory phase in BH task. LA, left anterior; LC, left central; LP, left posterior; MA, middle anterior; MC, middle central; MP, middle posterior; RA, right anterior; RC, right central; RP, right posterior.

In some specific areas associated with task engagement that are usually in the right hemisphere (42, 43) and in the α-band, which is commonly associated with higher arousal state (19), the results may be partially influenced by the task. However, the sinusoidal shape perfectly following the CO_2/O_2 behavior observed at the cross-correlation analysis even at RFP analysis seems again to conflict with this possible interpretation, at least with spatio-temporal resolution of the study. A way to explore this topic would be to ask the subject to think about performing a BH without actually doing it (no gas changes) or to perform the phase of normal breathing imposing a paced rhythm (both apnea and normal ventilation under voluntary control). Furthermore, focusing on specific areas known to be associated with task commitment and using high-resolution EEG may be of additive value in this respect.

The main novelty of the current study is surely represented by the analysis of RFP, which has never been performed so far either in BH studies or in experiments involving gas administration. This kind of analysis may help us to understand another relevant issue. Indeed, it is still not completely clear whether the cortical activation, which follows a gas challenge, would be mediated by the chemoreflex or related by a direct effect of hypercapnia or hypoxia on cortical neurons. Potentially, a change in the EEG activity may also derive from the vasodilatory effect due to hypercapnia and hypoxia. If the latter two hypotheses were correct, a rather uniform and homogeneous change in cortical activity would have emerged. On the contrary, looking at both the spectral maps and the RFP-related cross-correlations, a heterogeneous temporo-spatial distribution was found.

Another novelty of this study stands in the analysis of the temporal distribution of RFP responses to BH. Specifically, following an increase in $P_{ET}CO_2$, the first cortical areas that showed an increased activity were the middle central and middle anterior, with the wave of cortical activation then irradiating to other more lateral and posterior areas (see also Supplemental Video S1). The temporal trends observed in the δ-band are biologically plausible considering the neuroanatomy of the ascending pathways originating from the brain stem neural network (28, 29, 44, 45). The time delay must be interpreted as a phase shift between the CO_2 waveform and the EEG waveform. Whereas for the δ-band the time shift ranges from 2 to 9 s, the time shift is usually longer and narrower (14–16 s) for the α-band and might thus reflect a secondary variation from a hierarchical standpoint.

Finally, the correlation between $P_{ET}CO_2$ / $P_{ET}O_2$ and cortical activity is almost completely lost during FB across the different regions of interest. At most, the sign of the correlation (generally weak) is reverted in some cortical regions as compared with BH. Indeed, during wakefulness and in FB conditions, the pre-Bötzinger complex in brain stem acts as the pacemaker of respiration controlling respiratory motoneurons, respiratory muscles, and finally, pulmonary

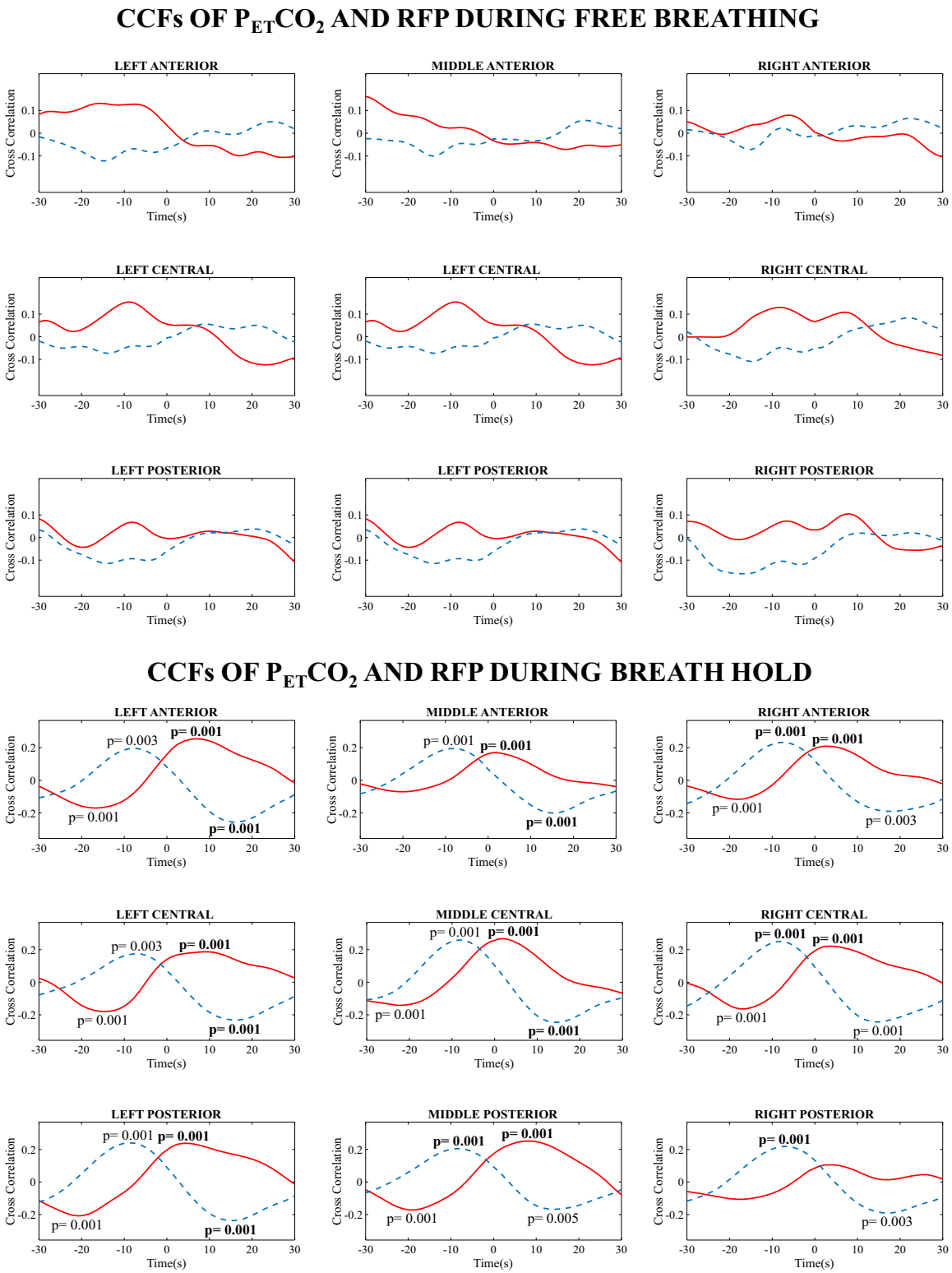

Figure 2. Time courses of the cross-correlation functions (CCFs) as a function of the time shift in free-breathing (FB) task and breath-hold (BH) task between 9 different brain areas (LA, left anterior; LC, left central; LP, left posterior; MA, middle anterior; MC, middle center; MP; middle posterior; RA, right anterior; RC, right central; RP, right posterior) and $P_{ET_{CO_2}}$. δ-Band results are reported in solid red lines, and α-band results are in dashed blue lines. *P* values are shown for maximum and minimum values of correlation. In bold are the strongest significant correlation coefficients. The critical values for significance after Benjamini-Yekuteli correction are p_crit = 0 for FB and p_crit = 0.041 for BH (4, 5).

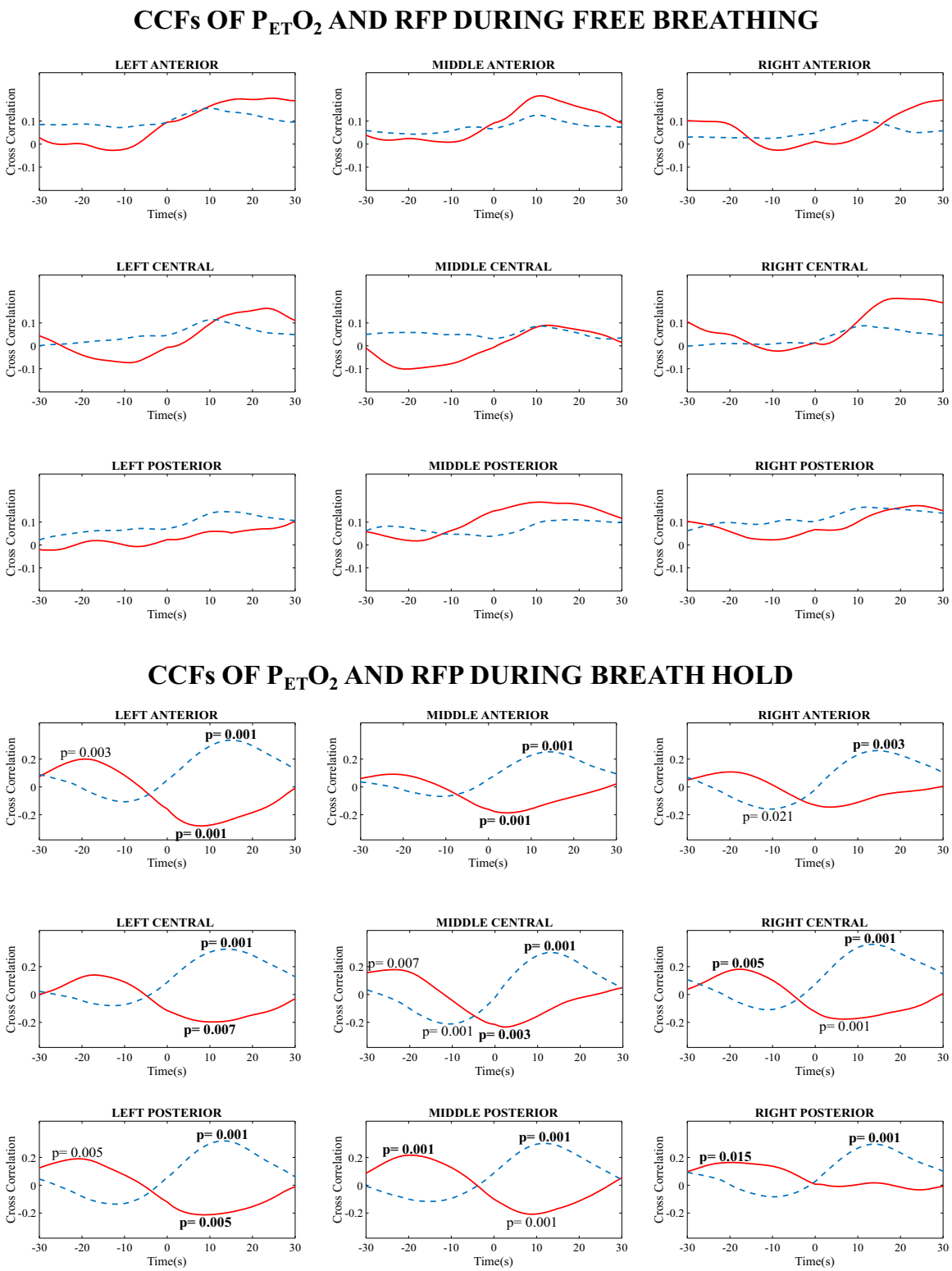

Figure 3. Time courses of the cross-correlation functions as a function of the time shift in free-breathing (FB) task and breath-hold (BH) task between 9 different brain areas (LA, left anterior; LC, left central; LP, left posterior; MA, middle anterior; MC, middle center; MP, middle posterior; RA, right anterior; RC, right central; RP, right posterior) and $P_{ET_{O_2}}$. δ-Band results are reported in solid red lines, and α-band results are in blue dashed lines. *P* values are shown for maximum and minimum values of correlation. In bold are the strongest significant correlation coefficients. The critical values for significance after Benjamini-Yekuteli correction are *p*_crit = 0 for FB and *p*_crit = 0.023 for BH (4, 5).

Table 2. *Correlation analysis results between regional field power and $P_{ET_{CO_2}}$ at the group level for 9 different brain areas*

	δ-Band			α-Band		
	T_s	CC	*P* value	T_s	CC	*P* value
Left anterior	7*	0.26*	0.001*	16*	-0.26*	0.001*
Middle anterior	2*	0.17*	0.001*	15*	-0.20*	0.001*
Right anterior	3*	0.21*	0.001*	−7*	0.23*	0.001*
Left central	9*	0.19*	0.001*	16*	-0.23*	0.001*
Middle central	2*	0.27*	0.001*	14*	-0.25*	0.001*
Right central	4*	0.22*	0.001*	−8*	0.25*	0.001*
Left posterior	4*	0.24*	0.001*	15*	-0.24*	0.001*
Middle posterior	8*	0.25*	0.001*	-8*	-0.21*	0.001*
Right posterior	3	0.11	0.05	−7*	0.22*	0.001*

T_s, time shift with maximum correlation coefficient; CC, correlation coefficient at T_s. *Significant maximum cross-correlation value. The critical *P* value at which cross-correlation was considered significant according to Benjamini-Krieger-Yekutieli false discovery rate correction was p_{crit} = 0.041.

ventilation, and it is poorly influenced by the chemoreflex (46). Therefore, any cortical activity related to, e.g., speaking, eating, or emotions (descending pathways) may cause variations in ventilation and thus in CO_2 and O_2 operating on the plant (lung) gain (47).

Study Limitations

EEG channel impedance was kept below 30 kΩ on average across subjects. This value is relatively high compared with the typical values, usually set below 10 kΩ. However, with modern high-input impedance amplifiers and accurate digital filters for power line noise, it has been demonstrated that high-quality EEG can be successfully recorded with impedance values up to 40 kΩ (48). Thus, considering the high-input impedance (>10 GΩ) of our EEG system and the homogeneity of the EEG signal across the different electrodes of the EEG cap for each subject, we are confident that the signal was accurately captured at the scalp surface. Furthermore, considering the group under study, all subjects had similar values of impedance, and we observed coherent cross-correlation courses. Finally, the quality of EEG signals was confirmed by highly experienced neurologists (M. Maestri and E. Bonanni).

The circulation delay related to the increase in venous CO_2 (metabolism), the transit through the lung, the delivery to the central nervous system, and the diffusion into the cerebrospinal fluid was not taken into account in this study. Indeed, this information is difficult to obtain in humans in vivo. Our group is currently developing novel methods to assess the circulatory time delay (A. Giannoni, D. Caratozzolo, F. Gentile, C. Borrelli, C. Taddei, E. Poggianti, C. Petersen, E. Pasanisi, M. Emdin, C. Passino, unpublished observations) in humans. These methods could be used in the future to correct for differences in cardiac output, especially when moving to patients in whom a greater variability in cardiac hemodynamic and circulatory delay is likely to occur. Moreover, the analysis of subcortical areas by deep source analysis or functional magnetic resonance imaging may help to understand some of these relevant questions.

Finally, in our study, we limited our observation to the effects of voluntary BH on GFP and RFP. We have not considered the motor component of the task or other possible effects such as respiratory sensation, which includes air hunger, chest tightness, effort of breathing, an urge to cough, urge to sneeze, and sense of suffocation (49). Indeed, respiratory sensation involves neural pathways in the pons, midbrain, hypothalamus, amygdala, cingulate, parahippocampal and fusiform gyrus anterior insula, presupplementary motor area, and middle frontal gyrus (49–51). In previous EEG studies, dyspnea was evaluated through variations of respiratory evoked potential elicited by inspiratory occlusion and inspiratory resistive load (52, 53). However, dyspnea was not a topic of interest in the current physiological study, and the duration of BH was short enough not to create discomfort in healthy subjects. Furthermore, subjects have been preliminarily trained to correctly perform the task, and the acquisitions did not begin until they were comfortable enough to perform BH. None of the subjects actually reported dyspnea or discomfort when executing the BH task, and therefore, we believe that the mental distress was rather low. Future studies could focus on this topic by either increasing BH duration or selecting the population in which the symptom is more likely to occur during a 30-s BH, such as patients with heart failure or chronic obstructive pulmonary disease.

Conclusions

In healthy subjects, a different behavior of $P_{ET_{CO_2}}$, $P_{ET_{O_2}}$, and EEG power is observed during the FB and BH tasks. During FB and in awake conditions, the cortex is sending signals to the brain stem, changing ventilation and causing subtle CO_2/O_2 variations. During BH task, the greater oscillatory changes in CO_2 and O_2 seem to cause consequent variation in cortical activity, with antiphase oscillation in the δ-band (positive correlation with CO_2, negative correlation with O_2) and in the α-band (negative correlation with CO_2, positive correlation with O_2). At regional analysis, a specific temporal pathway of cortical activation may be identified in the δ-band, with the earliest activation being observed centrally and a subsequent cortical propagation toward lateral and posterior regions with some delay. This seems to also apply to the α-band, which is suppressed in a heterogenous fashion but with longer delays as compared with the δ-band. This characteristic

Table 3. *Correlation analysis results between regional field power and $P_{ET_{O_2}}$ at the group level for nine different brain areas*

	δ-Band			α-Band		
	T_s	CC	*P* Value	T_s	CC	*P* Value
Left anterior	8*	−0.28*	0.001*	15*	0.34*	0.001*
Middle anterior	4*	−0.19*	0.001*	14*	0.25*	0.001*
Right anterior	3	−0.15	0.037	15*	0.26*	0.003*
Left central	10*	−0.20*	0.007*	14*	0.33*	0.001*
Middle central	2*	−0.23*	0.003*	13*	0.30*	0.001*
Right central	−18*	0.18*	0.005*	13*	0.36*	0.001*

T_s, time shift with maximum correlation coefficient; CC, correlation coefficient at T_s. *Significant maximum cross-correlation value. The critical *P* value at which cross-correlation was considered significant according to Benjamini-Krieger-Yekutieli false discovery rate correction was p_{crit} = 0.023.

behavior of cortical response to CO_2/O_2 variations could suggest a specific chemoreflex-mediated stimulation of the cortex through specific ascending pathways (especially in the δ-band) and also the presence of cortico-cortical interactions (δ-band changes preceding α-band changes). The latter point should be more deeply investigated in future studies, by using multivariate measures of brain connectivity, as partial directed coherence or directed transfer function, applied to brain sources (54–56). Furthermore, the investigation of subcortical sources integrating different methodologies, such as functional magnetic resonance imaging, could reveal the involvement of deep structures along with the corresponding pathways (57). These methodological advancements may be also exploited when designing future studies in which a specific group of chemoreceptor may be stimulated (i.e., reverse microdialisys or optogenetic stimulation in animals) or suppressed by specific drugs (also in humans) (8).

ACKNOWLEDGMENTS

The authors thank Dr. Giovanni Iudice and Dr. Francesca Bramanti (Fondazione Toscana Gabriele Monasterio of Pisa) for technical support.

DISCLOSURES

No conflicts of interest, financial or otherwise, are declared by the authors.

AUTHOR CONTRIBUTIONS

M.S.M., N.V., M.E., C.P. and A.G. conceived and designed research; M.S.M., N.V., A.L.C., V.H. and A.G. performed experiments; M.S.M., N.V., and A.L.C. analyzed data; M.S.M., N.V., M.M., E.B. and A.G. interpreted results of experiments; M.S.M. prepared figures; M.S.M. and A.G. drafted manuscript; M.S.M., N.V., A.L.C., V.H., M.M., E.B. and A.G. edited and revised manuscript; M.S.M., N.V., A.L.C., V.H., M.M., E.B., M.E., C.P. and A.G. approved final version of manuscript.

REFERENCES

1. **Herrero JL**, **Khuvis S**, **Yeagle E**, **Cerf M**, **Mehta AD.** Breathing above the brainstem: volitional control and attentional modulation in humans. *J Neurophysiol* 119: 145–159, 2018. doi:10.1152/jn.00551.2017.
2. **Feldman JL**, **Del Negro CA.** Looking for inspiration: new perspectives on respiratory rhythm. *Nat Rev Neurosci* 7: 232–242, 2006. doi:10.1038/nrn1871.
3. **Chapman SJ**, **Fowler AC**, **Hinch R.** Respiration. In: *An Introduction to Mathematical Physiology*. Mathematical Institute, Oxford University, 2010.
4. **Giannoni A**, **Emdin M**, **Poletti R**, **Bramanti F**, **Prontera C**, **Piepoli M**, **Passino C.** Clinical significance of chemosensitivity in chronic heart failure: influence on neurohormonal derangement, Cheyne-Stokes respiration and arrhythmias. *Clin Sci (Lond)* 114: 489–497, 2008. doi:10.1042/CS20070292.
5. **Geerling JC**, **Mettenleiter TC**, **Loewy AD.** Orexin neurons project to diverse sympathetic outflow systems. *Neuroscience* 122: 541–550, 2003. doi:10.1016/j.neuroscience.2003.07.008.
6. **Peyron C**, **Tighe DK**, **Van Den Pol AN**, **De Lecea L**, **Heller HC**, **Sutcliffe JG**, **Kilduff TS.** Neurons containing hypocretin (orexin) project to multiple neuronal systems. *J Neurosci* 18: 9996–10015, 1998. doi:10.1523/jneurosci.18-23-09996.1998. doi:10.1523/JNEUROSCI.18-23-09996.1998.
7. **Del Rio R**, **Marcus NJ**, **Schultz HD.** Carotid chemoreceptor ablation improves survival in heart failure: Rescuing autonomic control of cardiorespiratory function. *J Am Coll Cardiol* 62: 2422–2430, 2013. doi:10.1016/j.jacc.2013.07.079.
8. **Giannoni A**, **Borrelli C**, **Mirizzi G**, **Richerson GB**, **Emdin M**, **Passino C.** Benefit of buspirone on chemoreflex and central apnoeas in heart failure: a randomized controlled crossover trial. *Eur J Heart Fail*. 2020. doi:10.1002/ejhf.1854.
9. **McBryde FD**, **Abdala AP**, **Hendy EB**, **Pijacka W**, **Marvar P**, **Moraes DJA**, **Sobotka PA**, **Paton JFR.** The carotid body as a putative therapeutic target for the treatment of neurogenic hypertension. *Nat Commun* 4, 2013. doi:10.1038/ncomms3395.
10. **Narkiewicz K**, **Ratcliffe LEK**, **Hart EC**, **Briant LJB**, **Chrostowska M**, **Wolf J**, **Szyndler A**, **Hering D**, **Abdala AP**, **Manghat N**, **Burchell AE**, **Durant C**, **Lobo MD**, **Sobotka PA**, **Patel NK**, **Leiter JC**, **Engelman ZJ**, **Nightingale AK**, **Paton JFR.** Unilateral Carotid Body Resection in Resistant Hypertension: A Safety and Feasibility Trial. *JACC Basic to Transl Sci* 1: 313–324, 2016. doi:10.1016/j.jacbts.2016.06.004.
11. **Niewinski P**, **Janczak D**, **Rucinski A**, **Tubek S**, **Engelman ZJ**, **Piesiak P**, **Jazwiec P**, **Banasiak W**, **Fudim M**, **Sobotka PA**, **Javaheri S**, **Hart ECJ**, **Paton JFR**, **Ponikowski P.** Carotid body resection for sympathetic modulation in systolic heart failure: results from first-in-man study. *Eur J Heart Fail* 19: 391–400, 2017. doi:10.1002/ejhf.641.
12. **Pijacka W**, **Moraes DJA**, **Ratcliffe LEK**, **Nightingale AK**, **Hart EC**, **Da Silva MP**, **Machado BH**, **McBryde FD**, **Abdala AP**, **Ford AP**, **Paton JFR.** Purinergic receptors in the carotid body as a new drug target for controlling hypertension. *Nat Med* 22: 1151–1159, 2016. doi:10.1038/nm.4173.
13. **Bloch-Salisbury E**, **Lansing R**, **Shea SA.** Acute changes in carbon dioxide levels alter the electroencephalogram without affecting cognitive function. *Psychophysiology* 37: 418–426, 2000. doi:10.1111/1469-8986.3740418.
14. **Morelli M**, **Giannoni A**, **Passino C**, **Landini L**, **Emdin M**, **Vanello N.** A cross-correlational analysis between electroencephalographic and end-tidal carbon dioxide signals: methodological issues in the presence of missing data and real data results. *Sensors*, 16: 1828, 2016. doi:10.3390/S16111828. doi:10.3390/s16111828.
15. **Morelli MS**, **Greco A**, **Valenza G**, **Giannoni A**, **Emdin M**, **Scilingo EP**, **Vanello N.** Analysis of generic coupling between EEG activity and PETCO2 in free breathing and breath-hold tasks using Maximal Information Coefficient (MIC). *Sci Rep* 8: 4492, 2018. doi:10.1038/s41598-018-22573-6.]
16. **Thesen T**, **Leontiev O**, **Song T**, **Dehghani N**, **Hagler DJ**, **Huang M**, **Buxton R**, **Halgren E.** Depression of cortical activity in humans by mild hypercapnia. *Hum Brain Mapp* 33: 715–726, 2012. doi:10.1002/hbm.21242.
17. **Wang D**, **Piper AJ**, **Yee BJ**, **Wong KK**, **Kim JW**, **D'Rozario A**, **Rowsell L**, **Dijk DJ**, **Grunstein RR.** Hypercapnia is a key correlate of EEG activation and daytime sleepiness in hypercapnic sleep disordered breathing patients. *J Clin Sleep Med* 10: 517–522, 2014. doi:10.5664/jcsm.3700.
18. **Wang D**, **Yee BJ**, **Wong KK**, **Kim JW**, **Dijk D-J**, **Duffin J**, **Grunstein RR.** Comparing the effect of hypercapnia and hypoxia on the electroencephalogram during wakefulness. *Clin Neurophysiol* 126: 103–109, 2015. doi:10.1016/j.clinph.2014.04.012.
19. **Xu F**, **Uh J**, **Brier MR**, **Hart J**, **Yezhuvath US**, **Gu H**, **Yang Y**, **Lu H.** The influence of carbon dioxide on brain activity and metabolism in conscious humans. *J Cereb Blood Flow Metab* 31: 58–67, 2011. doi:10.1038/jcbfm.2010.153.
20. **Rau R**, **Raschka C**, **Brunner K**, **Banzer W.** Spectral analysis of electroencephalography changes after choking in judo (juji-jime). *Med Sci Sports Exerc* 30: 1356–1362, 1998. doi:10.1097/00005768-199809000-00003. doi:10.1249/00005768-199809000-00003, 10.1097/00005768-199809000-00003.
21. **Kastrup A**, **Li TQ**, **Glover GH**, **Moseley ME.** Cerebral blood flow-related signal changes during breath-holding. *AJNR Am J Neuroradiol* 20: 1233–1238, 1999.
22. **Giannoni A**, **Baruah R**, **Willson K**, **Mebrate Y**, **Mayet J**, **Emdin M**, **Hughes AD**, **Manisty CH**, **Francis DP.** Real-time dynamic carbon dioxide administration. *J Am Coll Cardiol* 56: 1832–1837, 2010. doi:10.1016/j.jacc.2010.05.053.

23. **Eckert DJ**, **Jordan AS**, **Merchia P**, **Malhotra A.** Central sleep apnea: Pathophysiology and treatment. *Chest* 131: 595–607, 2007. doi:10.1378/chest.06.2287.
24. **Eckert DJ**, **Malhotra A.** Pathophysiology of adult obstructive sleep apnea. *Proc Am Thorac Soc* 5: 144–153, 2008. doi:10.1513/pats.200707-114MG.
25. **Naughton MT.** Respiratory sleep disorders in patients with congestive heart failure. *J Thorac Dis* 7: 1298–1310, 2015. doi:10.3978/j.issn.2072-1439.2015.07.02.
26. **Rodin E**, **Funke M.** Cerebral electromagnetic activity in the subdelta range. *J Clin Neurophysiol* 23: 238–244, 2006. doi:10.1097/01.wnp.0000205161.22299.ea.
27. **Schellart NA**, **Reits D.** Voluntary breath holding affects spontaneous brain activity measured by magnetoencephalography. [Online]. *Undersea Hyperb Med* 26: 229–234, 1999. http://www.ncbi.nlm.nih.gov/pubmed/10642069 [21 Oct. 2015].
28. **Card JP**, **Sved JC**, **Craig B**, **Raizada M**, **Vazquez J**, **Sved AF.** Efferent projections of rat rostroventrolateral medulla C1 catecholamine neurons: implications for the central control of cardiovascular regulation. *J Comp Neurol* 499: 840–859, 2006. doi:10.1002/cne.21140.
29. **Guyenet PG**, **Stornetta RL**, **Souza GMPR**, **Abbott SBG**, **Shi Y**, **Bayliss DA.** The Retrotrapezoid Nucleus: Central Chemoreceptor and Regulator of Breathing Automaticity. *Trends Neurosci*. 42: 807–824, 2019. [doi:10.1016/j.tins.2019.09.002.
30. **Kosofsky BE**, **Mollive ME.** The serotoninergic innervation of cerebral cortex: Different classes of axon terminals arise from dorsal and median raphe nuclei. *Synapse* 1: 153–168, 1987. doi:10.1002/syn.890010204.
31. **Steinbusch HWM.** Distribution of serotonin-immunoreactivity in the central nervous system of the rat-Cell bodies and terminals. *Neuroscience* 6: 557–618, 1981. doi:10.1016/0306-4522(81)90146-9.
32. **Urigüen JA**, **Garcia-Zapirain B.** EEG artifact removal-state-of-the-art and guidelines. *J Neural Eng* 12: 31001, 2015. doi:10.1088/1741-2560/12/3/031001.
33. **McSwain SD**, **Hamel DS**, **Smith PB**, **Gentile MA**, **Srinivasan S**, **Meliones JN**, **Cheifetz IM.** End-tidal and arterial carbon dioxide measurements correlate across all levels of physiologic dead space. *Respir Care* 55: 288–293, 2010. doi:10.1136/emj.2010.092296.
34. **Simpson DM**, **Infantosi AFC**, **Botero Rosas DA.** Estimation and significance testing of cross-correlation between cerebral blood flow velocity and background electro-encephalograph activity in signals with missing samples. *Med Biol Eng Comput* 39: 428–433, 2001. doi:10.1007/BF02345364.
35. **Yuan H**, **Zotev V**, **Phillips R**, **Bodurka J.** Correlated slow fluctuations in respiration, EEG, and BOLD fMRI. *Neuroimage* 79: 81–93, 2013. doi:10.1016/j.neuroimage.2013.04.068.
36. **Glover T**, **Mitchell K.** An Introduction to Biostatistics: Third Edition [Online]. Waveland Press. https://books.google.com/books?id=v2B3CgAAQBAJ&pgis=1 [14 Mar 2016].
37. **Benjamini Y**, **Krieger AM**, **Yekutieli D.** Adaptive linear step-up procedures that control the false discovery rate. *Biometrika* 93: 491–507, 2006. doi:10.1093/biomet/93.3.491.
38. **Benjamini Y**, **Yekutieli D.** The control of the false discovery rate in multiple testing under dependency [Online]. *Ann Stat* 29: 1165–1188, 2001. https://www.jstor.org/stable/2674075?seq=1#metadata_info_tab_contents [23 Oct. 2020].
39. **Theiler J**, **Eubank S**, **Longtin A**, **Galdrikian B**, **Farmer D.** Testing for nonlinearity in time series: the method of surrogate data. *Phys D Nonlinear Phenom* 58: 77–94, 1992. doi:10.1016/0167-2789(92)90102-S.
40. **Fabbrini M**, **Bonanni E**, **Maestri M**, **Passino C**, **Giannoni A**, **Emdin M**, **Varanini M**, **Murri L.** Automatic analysis of EEG pattern during sleep in Cheyne-Stokes respiration in heart failure. *Sleep Med* 12: 529–530, 2011. doi:10.1016/j.sleep.2011.03.005. [doi:10.1016/j.sleep.2011.03.005, 10.1016/S1389-9457(11)00140-7.
41. **Thomas RJ.** Arousals in sleep-disordered breathing: patterns and implications. *Sleep* 26: 1042–1047, 2003. [Mismatch]. doi:10.1093/sleep/26.8.1042.
42. **Bartolomeo P**, **Seidel Malkinson T.** Hemispheric lateralization of attention processes in the human brain [Online]. *Curr Opin Psychol* 29: 90–96, 2019. doi:10.1016/j.copsyc.2018.12.023.
43. **Weinberg WA**, **Harper CR.** Vigilance and its disorders. *Neurol Clin* 11: 59–78, 1993. http://www.ncbi.nlm.nih.gov/pubmed/8441374. doi:10.1016/S0733-8619(18)30170-1.
44. **Avesar D**, **Stephens EK**, **Gulledge AT.** Serotonergic regulation of corticoamygdalar neurons in the mouse prelimbic cortex. *Front Neural Circuits* 12: 63, 2018. doi:10.3389/fncir.2018.00063.
45. **Buchanan GF**, **Richerson GB.** Role of chemoreceptors in mediating dyspnea. *Respir Physiol Neurobiol* 167: 9–19, 2009. doi:10.1016/j.resp.2008.12.002.
46. **Garcia AJ 3rd**, **Zanella S**, **Koch H**, **Doi A**, **Ramirez JM.** Chapter 3—networks within networks: the neuronal control of breathing. *Prog Brain Research* 188: 31–50, 2011. doi:doi: . doi:10.1016/B978-0-444-53825-3.00008-5.
47. **Giannoni A**, **Gentile F**, **Navari A**, **Borrelli C**, **Mirizzi G**, **Catapano G**, **Vergaro G**, **Grotti F**, **Betta M**, **Piepoli MF**, **Francis DP**, **Passino C**, **Emdin M.** Contribution of the lung to the genesis of cheyne-stokes respiration in heart failure: Plant gain beyond chemoreflex gain and circulation time. *J Am Heart Assoc* 8: e012419, 2019. doi:10.1161/JAHA.119.012419.
48. **Ferree TC**, **Luu P**, **Russell GS**, **Tucker DM.** Scalp electrode impedance, infection risk, and EEG data quality. *Clin Neurophysiol* 112: 536–544, 2001. doi:10.1016/S1388-2457(00)00533-2.
49. **Davenport PW**, **Vovk A.** Cortical and subcortical central neural pathways in respiratory sensations. *Respir Physiol Neurobiol* 167: 72–86, 2009. doi:10.1016/j.resp.2008.10.001.
50. **Binks AP**, **Evans KC**, **Reed JD**, **Moosavi SH**, **Banzett RB.** The time-course of cortico-limbic neural responses to air hunger. *Respir Physiol Neurobiol* 204: 78–85, 2014. doi:10.1016/j.resp.2014.09.005.
51. **Brannan S**, **Liotti M**, **Egan G**, **Shade R**, **Madden L**, **Robillard R**, **Abplanalp B**, **Stofer K**, **Denton D**, **Fox PT.** Neuroimaging of cerebral activations and deactivations associated with hypercapnia and hunger for air. *Proc Natl Acad Sci U S A* 98: 2029–2034, 2001. doi:10.1073/pnas.98.4.2029.
52. **Raux M**, **Navarro-Sune X**, **Wattiez N**, **Kindler F**, **Le Corre M**, **Decavele M**, **Demiri S**, **Demoule A**, **Chavez M**, **Similowski T.** Adjusting ventilator settings to relieve dyspnoea modifies brain activity in critically ill patients: an electroencephalogram pilot study. *Sci Rep* 9: 1–10, 2019. doi:10.1038/s41598-018-37186-2.
53. **Von Leupoldt A**, **Bradley MM**, **Lang PJ**, **Davenport PW.** Neural processing of respiratory sensations when breathing becomes more difficult and unpleasant. *Front Physiol* 1: 144, 2010. doi:10.3389/fphys.2010.00144.
54. **Bastos AM**, **Schoffelen JM.** A tutorial review of functional connectivity analysis methods and their interpretational pitfalls. *Front Syst Neurosci* 9: 175, 2016. doi:10.3389/fnsys.2015.00175.
55. **Callara AL**, **Morelli MS**, **Hartwig V**, **Landini L**, **Giannoni A**, **Passino C**, **Emdin M**, **Vanello N.** Ld-EEG effective brain connectivity in patients with Cheyne-Stokes respiration. *IEEE Trans Neural Syst Rehabil Eng* 28: 1216–1225, 2020. doi:10.1109/TNSRE.2020.2981991.
56. **Faes L**, **Nollo G.** Multivariate Frequency Domain Analysis of Causal Interactions in Physiological Time Series. In: *Biomedical Engineering, Trends in Electronics, Communications and Software*. InTech, 2011.
57. **Rosa MJ**, **Daunizeau J**, **Friston KJ.** EEG-fMRI integration: a critical review of biophysical modeliing and data analysus approaches. *J Integr Neurosci* 09: 453–476, 2010. doi:10.1142/S0219635210002512.